

## Direct Observation of Electron Spin Density on TDAE Cations in the Ferromagnetic State of Solid TDAE-C<sub>60</sub>

Y. Deligiannakis, G. Papavassiliou, M. Fardis, G. Diamantopoulos, and F. Milia

*Institute of Materials Science, National Center for Scientific Research (NCSR) "Demokritos," 153 10 Aghia Paraskevi, Attikis, Greece*

C. Christides

*Department of Engineering Sciences, School of Engineering, University of Patras, 26110 Patras, Greece*

K. I. Pokhodnia and V. Barchuk

*Institute of Semiconductors, Ukrainian Academy of Sciences, Nauki Avenue 45, Kiev 252650, Ukraine*

(Received 15 January 1999; revised manuscript received 7 April 1999)

<sup>14</sup>N electron spin echo envelope modulation (ESEEM) and <sup>1</sup>H nuclear magnetic resonance (NMR) techniques have been employed in order to measure the unpaired electron spin density of amino nitrogens and CH<sub>3</sub> protons, in the low temperature ferromagnetic state of solid TDAE-C<sub>60</sub>. Well resolved <sup>14</sup>N ESEEM patterns were obtained for the first time below 9 K, and their analysis reveals an extremely low unpaired electron spin density on specific TDAE nitrogen sites. Also, <sup>1</sup>H NMR line shape measurements corroborate a stepwise increase of the electron spin density on the CH<sub>3</sub> protons below 9 K that is accompanied by the onset of an activated law for <sup>1</sup>H 1/T<sub>1</sub> with temperature.

PACS numbers: 75.50.Dd, 75.90.+w

One of the most intriguing problems in the field of molecular magnetism concerns the nature of the ferromagnetic (FM) behavior of the charge transfer compound TDAE-C<sub>60</sub> (TDAE = tetrakis dimethyl amino ethylene) below the [1]  $T_c \approx 16$  K. Since the initial report by Allemand *et al.* [2] the low temperature phase of TDAE-C<sub>60</sub> has been proposed to be itinerant FM [2], spin glassy [3], spin canted FM [4], and recently 3D Heisenberg FM [5,6]. All of these studies indicate that there are still many controversial aspects concerning the intrinsic nature of the FM interactions in TDAE-C<sub>60</sub>.

Specifically, although cations and anions are expected to carry unpaired spin density, only one line appears in the electron spin resonance (ESR) spectrum of TDAE-C<sub>60</sub> well above  $T_c$ . This might indicate that either the TDAE<sup>+</sup> signal is masked by the C<sub>60</sub><sup>-</sup> ESR line or that C<sub>60</sub><sup>-</sup> and TDAE<sup>+</sup> spins are strongly exchange coupled [7]. Alternatively, the electronic properties of TDAE-C<sub>60</sub> can be driven by spin cancellation, spin density wave, or charge density wave mechanisms [8]. This assertion is supported by ultraviolet and x-ray photoelectron experiments on TDAE-C<sub>60</sub>, which are consistently interpreted only by considering coexistence of TDAE<sup>0</sup> and TDAE<sup>2+</sup> states [9]. Besides, x-ray diffraction measurements have shown that the unit cell consists of two subcells, stacked in the *c* direction, whereas both TDAE molecules shift along the *b* axis by 0.02 Å [4]. This crystal structure is consistent with charge separation (TDAE<sup>+</sup> + TDAE<sup>+</sup> → TDAE<sup>0</sup> + TDAE<sup>2+</sup>) and can be correlated with a Peierls transition along the *c* direction of TDAE-C<sub>60</sub>.

Differences of the unpaired electron spin density, due to strong exchange coupling or charge separation, are very difficult to detect on C<sub>60</sub> because the spin density

is distributed over 60 carbon atoms. However, the spin density ( $\rho$ ) on TDAE is more localized (the spin density is mainly located on the central  $N_2C = N_2C$  fragment in free TDAE<sup>+</sup>, with a  $\rho \approx 0.135$  on nitrogen [10,11]) and it can be measured with the help of magnetic resonance techniques, via the <sup>14</sup>N and <sup>1</sup>H hyperfine interactions described by the Hamiltonian:  $H = S \cdot \hat{A} \cdot I$  ( $S, \hat{A}$  are the electronic and nuclear spin, respectively, and  $\hat{A}$  is the hyperfine coupling tensor). So far, no hyperfine structure has been observed with continuous-wave (CW) ESR in solid TDAE-C<sub>60</sub>. On the other hand, pulsed ESR techniques allow the detection of fine details in overlapping or inhomogeneous broadened signals with different phase memory, or spin-lattice relaxation times [12]. Another possibility is the use of electron spin echo envelope modulation (ESEEM) techniques, which can resolve low nuclear spin resonance frequencies of nuclei coupled with the electron spin [13]. Specifically, in TDAE-C<sub>60</sub> ESEEM can provide direct information about the <sup>14</sup>N and <sup>1</sup>H hyperfine coupling tensors.

In this Letter we report a detailed ESEEM and <sup>1</sup>H NMR study of TDAE-C<sub>60</sub> at low temperatures and give for the first time a direct experimental estimation of the unpaired electron spin density distribution on amino nitrogens and CH<sub>3</sub> protons of TDAE. Measurements have been carried out on a set of small, randomly oriented, TDAE-C<sub>60</sub> single crystals, which were grown at room temperature with a diffusion technique previously developed for low-dimensional organic conductors [14]. Freshly grown crystals were vacuum sealed in quartz tubes and x-ray diffraction measurements showed the absence of any significant inclusion of solvent, while the derived crystallographic parameters were similar to those

reported in Ref. [4]. Pulsed ESR measurements were performed at Commissariat à l'Energie Atomique Saclay (France) on a Bruker ESP 380 spectrometer, and  $^1\text{H}$  nuclear magnetic resonance (NMR) measurements have been carried out at NCSR Demokritos on a Bruker MSL spectrometer operating at 200 MHz  $^1\text{H}$  frequency.

Figure 1 demonstrates echo-detected field swept ESR spectra of TDAE- $\text{C}_{60}$  in the temperature interval between 4 and 21 K. All spectra were obtained by recording the amplitude of the echo as a function of the magnetic field after a two pulse sequence ( $\pi/2$ -144 ns- $\pi$ ), with a time duration of the  $\pi/2$  and  $\pi$  pulses, 32 and 64 ns, respectively. At 4 K, the spectrum consists of a strong central line at 3487 G, and two symmetrically disposed weak lines, which might be attributed to a  $\text{CH}_3$ -proton hyperfine splitting of about 25 G. An alternative explanation for the observed structure is the presence of  $^1\text{H}$  nuclear modulation in the ESR spectra, with period 5 G, due to strong  $\text{C}_{60}^-$ -proton hyperfine interactions [15]. Nevertheless, in both cases the conclusive factor for the observed structure is the presence of strong hyperfine interactions. By increasing temperature, the intensity of the three lines decreases rapidly, and the two outer lines disappear at 9 K (Fig. 1 inset). Above 9 K the central line continues to reduce on heating and disappears at about 16 K, due to the rapid decrease of the phase memory time on approaching  $T_c$  [16]. The resonance field of the ESR spectra varies only slightly with temperature below 16 K, indicating that the set of randomly oriented single crystals behaves like a polycrystalline sample. Thus the low frequency FM resonance mode, recently reported [5,6] in the radio frequency region, is not expected to create a

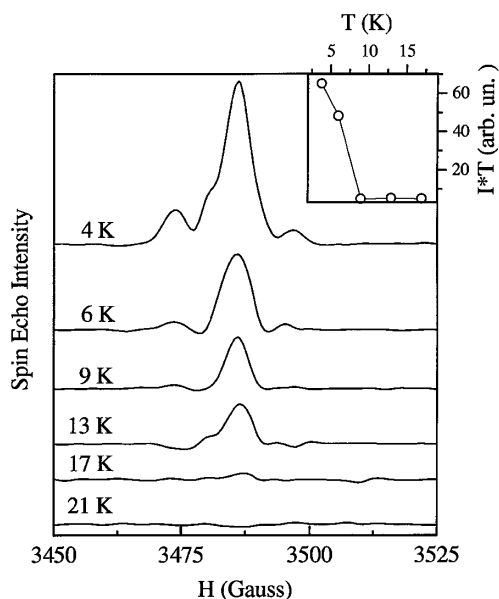


FIG. 1. Spin echo field swept ESR spectra of TDAE- $\text{C}_{60}$  at selected temperatures. The inset shows the stepwise increase of the Boltzmann corrected intensity  $IT$  vs  $T$  of the hyperfine pattern.

resonance field shift or a detectable signal distortion in the X band.

To resolve the hidden  $^1\text{H}$  and  $^{14}\text{N}$  hyperfine couplings under the central ESR signal ESEEM spectroscopy was used. Two ESEEM experiments were performed [17] at 4 and 6 K. It was impossible to obtain a well resolved ESEEM pattern above 8 K. Figure 2a displays the stimulated echo envelope modulation in the time domain at 6 K, at a field of 3487 G. There was no evidence of orientation selectivity, while the field dependence of the Larmor frequency across the spectrum did not cause significant alteration in the ESEEM pattern. The frequency-domain spectrum, obtained by Fourier transform of the time domain ESEEM pattern, is shown in Fig. 2b. The experimental spectrum contains a multiplex of sharp lines between 0.5 and 6 MHz, arising from  $^{14}\text{N}$ - $\text{C}_{60}^-$  coupling. Simulations of the  $^{14}\text{N}$  ESEEM spectra in the time and frequency domain [18] are also presented in Figs. 2a and 2b. The  $^{14}\text{N}$  peaks are nicely fitted with two sets of triplets, with relatively shifted axial hyperfine coupling tensors  $\hat{A}$ . In this model the  $\hat{A}$  tensor was written

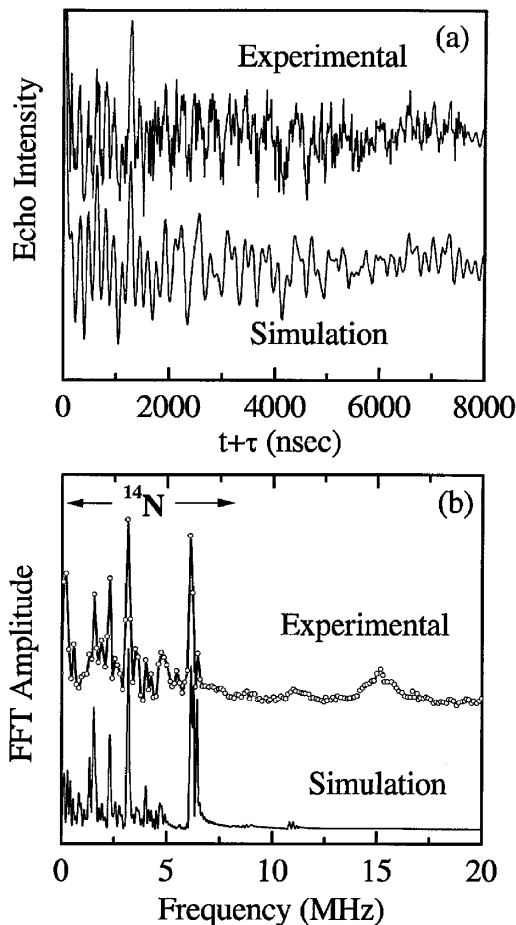


FIG. 2. (a) ESEEM of TDAE- $\text{C}_{60}$  at 6 K in the time domain and (b) the corresponding frequency domain spectrum. The lower graphs show the simulations of the  $^{14}\text{N}$  ESEEM.

as  $(A_{\text{iso}} - \tilde{T}, A_{\text{iso}} - \tilde{T}, A_{\text{iso}} + 2\tilde{T})$ , with the isotropic coupling  $A_{\text{iso}} = 2.27$  and  $3.2$  MHz and its anisotropic components  $\tilde{T} = 0.13$  and  $0.2$  MHz, respectively. These  $A_{\text{iso}}$  values correspond to  $\sigma$  spin density values  $0.0013$  and  $0.0018$ , respectively [19]. Alternatively, the obtained  $A_{\text{iso}}$  values can be attributed to  $\pi$  spin density on the nitrogen by using the formula [10]  $A_{\text{iso}} = Q\rho_{\pi}$  ( $Q \approx 31.8$  for TDAE-C<sub>60</sub>), which gives  $\rho_{\pi} \approx 0.07$  and  $0.1$ , respectively. However, such large  $\pi$  spin density values should produce large hyperfine anisotropy [20], which does not concur with the restricted anisotropy of the hyperfine tensor observed with ESEEM. Thus, the observed electron spin density on the nitrogens is of the  $\sigma$  type. At  $4$  K the  $^{14}\text{N}$  modulation depth is severely reduced due to the high value of  $A_{\text{iso}}$ , that is, estimated to be greater than  $5$  MHz.

Except the lower-frequency  $^{14}\text{N}$  peaks, a narrow peak at  $14.8$  MHz (this is the  $^1\text{H}$  nuclear Larmor frequency in external field of  $3487$  G) appears together with a weak broad doublet disposed symmetrically around the  $14.8$  MHz in ESEEM spectra. The frequency split of the doublet is about  $2$  to  $3$  MHz, in agreement with the  $^1\text{H}$  NMR results shown below. Another interesting feature appears at about  $11$  MHz in Fig. 2b. According to our analysis this peak appears as a weak contribution from a doublet of  $^{14}\text{N}$  lines in the simulated spectrum (Fig. 2b). However, the large disagreement between the calculated and Fourier transformed peak shapes at  $11$  MHz indicate that this feature may arise by  $^1\text{H}$  hyperfine couplings corresponding to an  $A_{\text{iso}} \approx 8$  MHz.

To investigate this possibility detailed  $^1\text{H}$  NMR line shape measurements were performed below  $16$  K. Characteristic spectra at  $1.8$ ,  $6$ ,  $10$ , and  $14$  K are shown in Fig. 3. These spectra exhibit the two lines previously reported [21]: one that remains unshifted ( $NS$  line) down to the lowest measured temperature and one that shifts rapidly on cooling ( $S$  line). Below  $9$  K the  $S$  line intensity increases abruptly (Fig. 3 inset), exhibiting a frequency shift up to  $8$  MHz, with unpaired electron spin density on  $S$ -type protons in the range of  $0.0028$  up to  $0.0056$  [19]. Apparently the three  $^1\text{H}$  NMR peaks with shifts  $0$ ,  $3$ , and  $8$  MHz correspond to the  $^1\text{H}$  ESEEM peaks at  $14.8$  MHz, the  $3$  MHz broad doublet, and the weak feature at  $11$  MHz, respectively [22]. This effect is observed for the first time in the present experiment and correlates with the  $\text{C}_{60}^-$ -proton hyperfine coupling that shows up in the field swept ESR spectra (Fig. 1 inset) below  $9$  K. Such correlation may imply that the unpaired spin density on the methyl protons is due to extension of the  $\text{C}_{60}^-$  unpaired electron wave function on the TDAE molecule. Remarkably, the onset of the  $S$  line broadening coincides with the formation of a nonzero spin gap, observed [23] by  $^1\text{H}$  spin-lattice relaxation rate  $1/T_1$  and CW ESR measurements in appropriately prepared nonferromagnetic TDAE-C<sub>60</sub> single crystals [24]. However, in these crystals only the  $NS$  line was observed. To in-

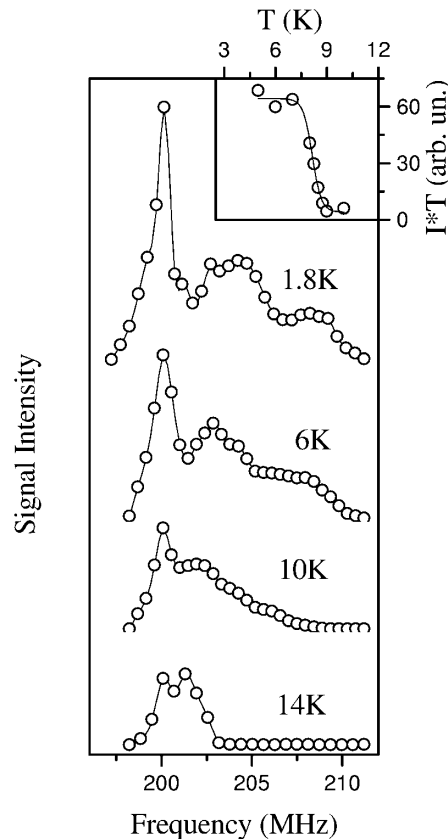


FIG. 3.  $^1\text{H}$  NMR spectra of TDAE-C<sub>60</sub> at  $1.8$ ,  $6$ ,  $10$ , and  $14$  K. For clarity the spectra are not scaled. The inset shows the stepwise increase of the Boltzmann corrected signal intensity  $IT$  vs  $T$ , at  $208$  MHz.

vestigate this effect in our sample,  $^1\text{H}$   $T_1$  versus  $T$  measurements were performed on the  $S$  and  $NS$  lines below  $16$  K. It is observed that  $(T_1T)^{-1}$  (Fig. 4) of the  $S$  line decreases rapidly below  $9$  K, providing evidence about the formation of a spin gap [25]. This is clearly shown in the semilog plot of  $1/T_1$  versus  $1000/T$  (Fig. 4 inset), where the  $1/T_1$  follows an activated law:  $1/T_1 \propto \exp(-E_T/kT)$  below  $9$  K, corresponding to an energy gap of  $E_T/k \approx 18$  K. This value is close to the energy gap value of  $E_T/k \approx 19$  K obtained [23] by  $^1\text{H}$  NMR on the nonferromagnetic modification of TDAE-C<sub>60</sub>. However, in our sample the  $1/T_1$  of the  $NS$  line does not follow an activation energy law. This may indicate that the  $S$  line protons in our sample and the protons exhibiting the spin gap behavior reported in Ref. [23] belong to stereochemically equivalent  $\text{CH}_3$  groups.

The above results indicate that at  $9$  K an inhomogeneous spin order might be overimposed to the FM state along the  $c$  axis. This picture is in conjunction with recent calculations by Sato *et al.* [8], indicating that the ground state of TDAE-C<sub>60</sub> is FM with the electronic structure  $\text{TDAE}^0(\uparrow)-\text{C}_{60}^-(\uparrow)-\text{TDAE}^{2+}-\text{C}_{60}^-(\uparrow)$ . Based on this model, the low  $\rho(^{14}\text{N}) \approx 0.0013$  and  $0.0018$  spin density values obtained with ESEEM at

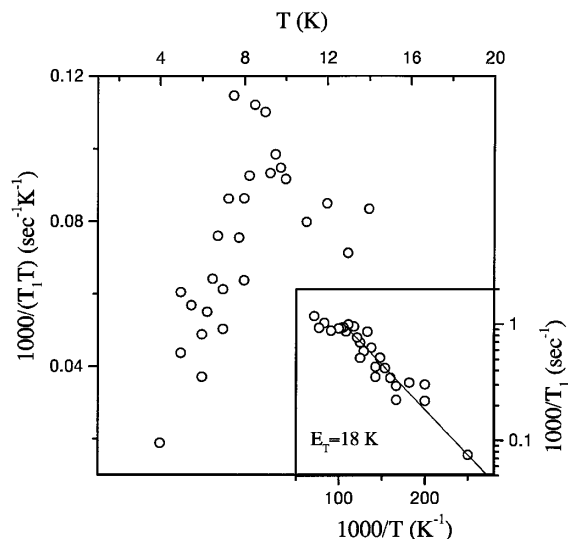


FIG. 4.  ${}^1\text{H}$   $1/T_1 T$  of TDAE- $\text{C}_{60}$  below 16 K, measured by standard saturation recovery methods on the  $S$  line. The inset shows the  $1/T_1$  vs  $1000/T$  in a semilog scale.

6 K can be attributed to spin cancellation on specific TDAE sites. Nevertheless, a mixed charge transferred state,  $(\text{TDAE}^0\text{-C}_{60}^{\ominus}\text{-TDAE}^{2+}\text{-C}_{60}^{\ominus})$  and  $(\text{TDAE}^0\text{-C}_{60}^0\text{-TDAE}^+\text{-C}_{60}^{\ominus})$ , cannot be excluded [8] because high spin density values of  $\rho({}^{14}\text{N}) \approx 0.1$  are not detectable by three-pulse ESEEM, but only with HYSORE [26].

In conclusion,  ${}^{14}\text{N}$  ESEEM and  ${}^1\text{H}$  NMR measurements on solid TDAE- $\text{C}_{60}$  have shown (i) the presence of a very low unpaired electron spin density on specific nitrogens, which are predicted in a model considering charge separation [8,9], (ii) an abrupt increase of the spin density on  $S$ -line  $\text{CH}_3$  protons below 9 K, and (iii) the formation of a spin gap below 9 K resulting from  ${}^1\text{H}$   $1/T_1$  measurements. The above results, together with the pseudo-one-dimensional magnetic structure of TDAE- $\text{C}_{60}$  and the antiferromagnetic correlations reported [4] along the  $c$  axis, may imply that a spin and charge density wave is superimposed on the FM state below 9 K.

This work has been supported by the NATO linkage Grant No. SA, 12-3-02(HTECHLG-960976) 1300(96)JARC-412.

- [1] A. Lappas *et al.*, *Science* **267**, 1799 (1995).  
 [2] P. M. Allemand *et al.*, *Science* **253**, 301 (1991).  
 [3] P. Cevc *et al.*, *Solid State Commun.* **90**, 543 (1994).  
 [4] R. Blinc *et al.*, *Phys. Rev. Lett.* **76**, 523 (1996).

- [5] D. Arcon *et al.*, *Phys. Rev. Lett.* **80**, 1529 (1998).  
 [6] R. Blinc *et al.*, *Phys. Rev. B* **58**, 14416 (1998).  
 [7] B. Gotschy, *Phys. Rev. B* **52**, 7378 (1995); B. Gotschy *et al.*, *Synth. Met.* **77**, 287 (1996).  
 [8] T. Sato *et al.*, *Phys. Rev. B* **56**, 307 (1997).  
 [9] S. Hino *et al.*, *J. Phys. Chem. A* **101**, 4346 (1997).  
 [10] K. Tanaka *et al.*, *J. Phys. Chem.* **100**, 3980 (1996).  
 [11] K. I. Pokhodnia *et al.*, *J. Chem. Phys.* **110**, 3606 (1999).  
 [12] M. Mehring *et al.*, *Solid State Commun.* **45**, 1075 (1983).  
 [13] S. A. Dikanov and Y. D. Tsvetov, *ESEEM Spectroscopy* (CRC Press, Boca Raton, FL, 1992).  
 [14] H. J. Guggenheim and D. Bahnck, *J. Cryst. Growth* **26**, 29 (1974).  
 [15] D. J. Goldfarb and L. Kevan, *J. Magn. Reson.* **76**, 276 (1988).  
 [16] P. Cevc *et al.*, *Europhys. Lett.* **26**, 707 (1994).  
 [17] In a standard three-pulse  $(\pi/2-t-\pi/2-\tau-\pi/2)$  ESEEM experiment the amplitude of the stimulated echo is recorded as a function of  $\tau$ . In our experiments the minimum interpulse  $\tau$  was 160 ns and was incremented in steps of 8 ns. The duration of the  $\pi/2$  pulses was 16 ns, corresponding to  $B_1 = 6$  G.  
 [18] Simulated spectra have been derived on the basis of the Hamiltonian,  $H = g\mu_B B_0 S_z - g_N \mu_N B_0 I_z + S \cdot \hat{A} \cdot I + I \cdot \hat{Q} \cdot I$ , where the first and the second terms are the electronic and the nuclear Zeeman terms, respectively, the third is the hyperfine interaction term, and the fourth the quadrupolar term for nuclei with  $I > 1/2$ . The three-pulse modulations were calculated by using the relations derived by Mims [W. B. Mims, *Phys. Rev. B* **5**, 2409 (1972); **6**, 3543 (1972)].  
 [19] One  $s$  electron produces a hyperfine coupling of 1420 MHz on the proton and 1811 MHz on the nitrogen. Thus the calculation of the normalized  $\sigma$  spin density is straightforward.  
 [20] J. R. Morton and K. F. Preston, *J. Magn. Reson.* **30**, 577 (1978).  
 [21] D. Arcon *et al.*, *Phys. Rev. B* **53**, 14028 (1996).  
 [22] A multiple-Gaussian fitting on the  ${}^1\text{H}$  ESEEM and NMR spectra (Figs. 2 and 3) at 6 K, gives the ratio of the signal intensities  $I(NS)/I(S) \approx 2.2$  from ESEEM, and  $\approx 2.5$  from NMR.  
 [23] D. Arcon *et al.*, *Phys. Rev. B* **59**, 5247 (1999).  
 [24] TDAE- $\text{C}_{60}$  samples prepared at room temperature consist of a mixture of ferromagnetic and nonferromagnetic modifications [23]. Below 9 K the ESR signal of the nonferromagnetic modification is negligibly small and does not influence the ESEEM analysis presented in this paper [23]. On the other hand, the ESR signal from the ferromagnetic modification increases significantly below  $T_c$  [K. Tanaka *et al.*, *Phys. Lett.* **164**, 221 (1992)].  
 [25] V. Brouet *et al.*, *Phys. Rev. Lett.* **82**, 2131 (1999).  
 [26] Y. Deligiannakis and A. W. Rutherford, *J. Am. Chem. Soc.* **119**, 4471 (1997).